

Comparative investigation of lattice-matched ternary and quaternary barriers for GaN-based HEMTs

S.Riedmüller^{1,2,#}, J. Grünenpütt¹, M. Madel¹, and H. Blanck¹

¹ United Monolithic Semiconductors GmbH, Wilhelm-Runge-Straße 11, 89081 Ulm, Germany

² Inst. of Functional Nanosystems University of Ulm, Albert-Einstein-Allee 45, 89081 Ulm, Germany

e-mail Sandra.riedmueller@ums-ulm.de, Phone: +49 731 505 3048

Keywords: AlIn(Ga)N/AlN/GaN HEMTs, band structure calculations

Abstract

In this paper we present the comparison of a HEMT structure based on ternary to that of quaternary AlIn(Ga)N large band gap material. Band profile simulations have been performed to study systematically the formation of a two-dimensional electron gas (2DEG). The processed devices with 120-nm gate length based on quaternary material exhibit 28 % less drain current and 30 % higher contact resistance compared to the AlInN/AlN/GaN HEMT. In addition, the gate leakage level was found to be a factor of 3 higher compared to the ternary material. Further reduction of leakage below 1 mA/mm was realized with a reduced AlInN barrier thickness achieving, thus a high output power density of 3.7 W/mm and a power added efficiency of 58 % at 9 GHz.

INTRODUCTION

For some time, high electron mobility transistors (HEMTs) based on AlGaIn/AlN/GaN heterostructures have attracted considerable attention for high-power and high-frequency applications [1]. Further improvement of HEMT performance can be reached by increasing the Al content in the barrier layer at the cost of strain-induced defects such as misfit dislocations and cracks caused by large lattice mismatch [2]. These effects limit the possible Al content to values below 40 % with barrier thicknesses above 15 nm [3]. To overcome such problems, the AlGaIn barrier layer can be replaced by ternary AlInN, which can be grown lattice-matched to GaN at an InN mole fraction of 17 %. Indeed, the high sheet charge densities in AlInN up to $3 \times 10^{13} \text{ cm}^{-2}$ induced by high spontaneous polarization [4], enable the use of a thinner barrier layer while keeping a high sheet carrier concentration at the interface. In order to achieve high frequency performance, thin barriers are a requirement for GaN-based HEMTs with down-scaled gate length. It is important to maintain a high aspect ratio of gate length to barrier thickness [5]. Although impressive results on AlInN barrier HEMTs have been reported [6], severe challenges remain for AlInN epitaxy. The large difference in In-N and Al-N bonding energies and the lack of miscibility of InN and AlN result in the appearance of inhomogeneities and extended

defects. This leads to a reduced mobility in the 2DEG compared to AlGaIn/GaN heterostructures [7]. In spite of the outstanding electrical performance values that have been demonstrated for this material system [8], material quality can affect and limit device reliability. In addition, the effect of unintentional Ga incorporation to the AlInN layer has been reported [9], which has been associated with the residual Ga in the growth chamber or diffusion from the GaN layer [10]. Imprecise Ga incorporation into the barrier material can change the structural, morphology and material properties giving rise to unwanted electrical characteristics. It has been predicted that AlInGaIn quaternaries have a narrower miscibility gap in the AlN-InN phase diagram than ternary alloys with the exception of AlGaIn [11]. This narrower gap results in decreased surface roughness and alloy scattering [12]. Both barrier materials can be grown lattice-matched to GaN with an In to Al ratio of 1:5 [13]. Consequently, the lattice-matched growth of quaternary barrier material results in smaller band gap energies compared to AlInN [12] and a reduced sheet carrier concentration in the 2DEG. In this paper we will investigate the effect these differences in band gap energies and sheet carrier concentration has on the final device to give a recommendation for a material layer stack appropriate for small gate length devices.

EXPERIMENTAL

In this letter we take a comparison of electrical results at the end of device processing for both lattice-matched materials and calculate systematically the band profiles of AlIn(Ga)N/AlN/GaN HEMT structures with different thicknesses of the AlIn(Ga)N barrier. The band structure and the quantized energy states of the heterostructures were modelled by self-consistently solving the Schrödinger and Poisson equations using Nextnano software. The AlIn(Ga)N/AlN/GaN heterostructures were grown on 4'' SiC substrates. A thin AlN interlayer was grown between barrier and GaN buffer for optimized carrier mobility. The Ga composition in the ternary barrier was lower than 1 % confirmed by XPS measurements. The AlInGaIn containing a nominal Ga content of 10 % was deposited at higher temperatures compared to AlInN. AFM was employed to evaluate the surface morphology (Fig. 1). A rather rough and

grainy morphology could be observed for the ternary material. In contrast, the quaternary material showed a rather smooth and step-like morphology. Hall measurements from the epitaxy supplier result in 11 % higher electron mobility for the quaternary barrier and 31 % lower 2DEG density compared to AlInN. The miscibility of AlInN improves with increasing Ga concentration and enables higher deposition temperatures resulting in better structural quality [14]. This result is shown in good agreement with those shown in a number of papers reporting higher mobilities in quaternary barrier HEMTs than in ternary HEMTs with similar design [3, 15, 16]. The low electron density in the 2DEG for the quaternary material can be explained by a smaller band gap energy for lattice- matched grown quaternary material.

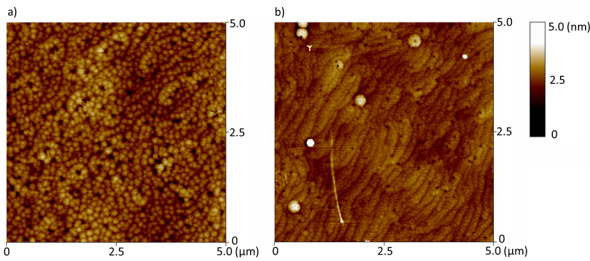


Fig. 1. $5 \times 5 \mu\text{m}^2$ AFM image of a) AlInN/AlN/GaN HEMT structure and b) AlInGaN/AlN/GaN HEMT structure.

RESULTS AND DISCUSSION

The conduction band profiles of the AlIn(Ga)N/AlN/GaN HEMTs from nextnano simulations are shown in Fig. 2. The AlInN HEMT structure showed a stronger distortion of the conduction band below the Fermi level.

As calculated from [12] and [17], the spontaneous polarization of AlInGaN is 0.6 C/m^2 which is 12 % less compared to AlInN. This results in a 15 % lower 2DEG density for AlInGaN. This was extracted for different barrier thicknesses from simulations performed with Nextnano (Fig. 3).

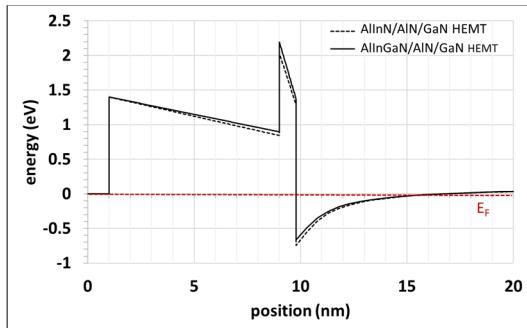


Fig. 2. Conduction band profile of the AlInN/AlN/GaN HEMT (dotted line) and of the AlInGaN/AlN/GaN HEMT (solid line).

The higher 2DEG density calculated for AlInN was fairly consistent with the Hall measurement results.

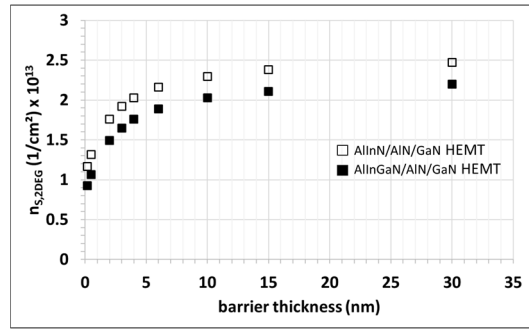


Fig. 3. Density of electrons in the 2DEG as a function of barrier thickness for ternary and quaternary structures.

To ensure the same surface properties a thin SiN passivation layer was deposited on top of the investigated heterostructures. Submicron GaN-based HEMTs were then fabricated by depositing a Ti/Al metallization sequence to form recessed Ohmic contacts followed by rapid thermal annealing. After ion implantation for device isolation, a transmission line measurement (TLM) was used to extract the Ohmic contact resistance. The transistor process was then completed through the realization of 120 nm T-shaped gates based on multi resist levels. Both material stacks were processed under the same conditions. To evaluate the influence of different materials on the transistor performance, the relevant electrical parameters were measured (Fig. 4).

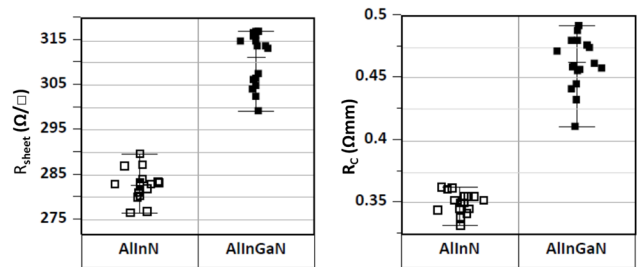


Fig. 4. Sheet resistance R_{sheet} and contact resistance R_c extracted from TLM measurements for samples with AlInN and AlInGaN barriers.

The ternary material has a lower sheet resistance compared to the quaternary material, which is consistent with Hall data. Ternary material also tends to show lower contact resistances.

The maximum drain saturation current I_{DS} and the maximum transconductance G_m for the ternary and quaternary material are shown in Fig. 5.

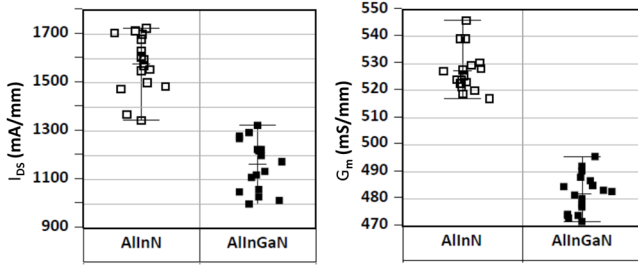


Fig. 5. Maximum drain saturation current I_{DS} and maximum transconductance G_m measured at $V_{GS} = -2$ V and $V_{DS} = 7$ V.

The lower sheet resistance observed for AllInN barrier material is reflected in 20 % more I_{DS} (1.6 A/mm). At 7 V drain bias, the maximum extrinsic transconductance for AllInN is 546 mS/mm. This value is 10 % higher than the maximum transconductance measured for the quaternary material. This difference in transconductance can be explained by the higher source resistance R_S observed for the quaternary material. To achieve a high extrinsic transconductance for this material system, the Ohmic contact has to be minimized.

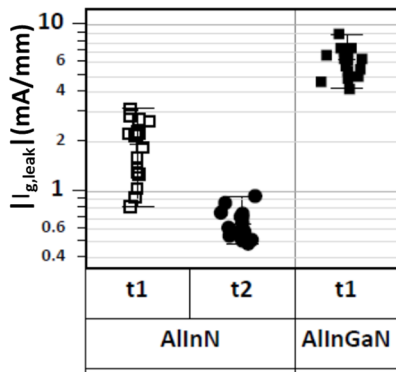


Fig. 6. Leakage current $I_{g,leak}$ for ternary and quaternary barrier material for different barrier thickness $t1$ and $t2$ at $V_{DS} = 7$ V.

Contradicting observations described in several papers [12, 15], the gate leakage current for AllInGaN is a factor of 3 higher than for AllInN with the same barrier thickness $t1$ (see Fig. 6). Further, higher leakage current for compounds closer to lattice-matched $Al_{0.83}In_{0.17}N$ was reported in [12] inducing a reduction of leakage current for quaternary compounds with increasing Ga content. In general, considering the electrical properties, better results were obtained as the amount of GaN increased in the AllInGaN alloy [18]. The discrepancy between these results presented in literature and this work may be explained with variations in, for example interface quality or defect density related to a non-ideal material quality. TEM investigations of different barrier materials grown on GaN were done in [18] and allocated that the quality of the interface between the GaN channel and spacer, as well as the crystalline quality of the barrier layer are roughly comparable and independent of the barrier composition. One

possible explanation for the higher leakage current for quaternary barrier material may lie in different surface states as well as in the access region or below the Schottky gate contact. However, pulse measurements result in similar gate- and drain-lag and indicate no noticeable current collapse for both materials.

To further lower the leakage level that may limit reliable device operation, an additional sample ($t2$) with 25% reduced AllInN barrier thickness was considered in order to reduce the 2DEG density by about 5%. Against the expectation based on Nextnano simulations, the 2DEG density measured by the epitaxy supplier dropped by more than 30%, which is confirmed by a lower maximum drain current density of 1100 mA/mm. SIMS analysis of the material is planned to identify whether the reason for this strong reduction in 2DEG density is epitaxy or process related. For instance, the surface passivation during the manufacturing process could be affecting the Fermi level pinning which is assumed to be constant at 1.4 eV in our simulations. Nevertheless, sample ($t2$) provides the same maximum drain current density as the quaternary devices but with a factor of 5 lower leakage level, thus achieving the goal of leakage level reduction.

Continuous-wave power measurements on an $8 \times 75 \mu\text{m}$ device were performed at $V_{DS} = 15$ V and a quiescent drain current density of $I_{DS} = 200$ mA/mm. The measurement results for transducer gain G_t , power added efficiency PAE and saturated RF output power P_{out} are shown in Table I.

TABLE I
LOADPULL MEASUREMENT AT 9 GHz, TRANSDUCER GAIN G_t ,
POWER ADDED EFFICIENCY PAE AND MAXIMUM OUTPUT
POWER P_{OUT} .

Material	Barrier thickness	G_t (dB)	PAE	P_{out} (W/mm)
AllInN	t1	13.2	59	4.9
AllInN	t2	14.3	58	3.7
AllInGaN	t1	13.7	56	3.5

All samples meet the minimum target at UMS for this technology of > 3 W/mm for the output power density. As expected from I_{DS} , the sample ($t2$) with thin AllInN barrier shows the same output power as the quaternary material. In addition, the thinner barrier also results in an increased RF gain compared to both other samples. Based on the higher gain and the lower leakage level, sample ($t2$) is the most promising candidate out of this experiment for further investigation and characterization.

CONCLUSIONS

The impact of ternary and quaternary barrier materials on the HEMT performance was studied. Band profile simulations have been performed using Nextnano software. The results are in very good agreement with Hall data and the experimental results. AFM measurements indicated a rather

smooth surface morphology for the quaternary material. The introduction of Ga into the barrier layer led to optimized material quality and improved electron mobility. Despite the rather rough surface morphology, the AlInN/AlN/GaN HEMT structure showed 28 % more drain current and lower contact resistance compared to the quaternary material. Contrary to previously published results, our experiments showed that lattice-matched AlInN yielded a reduced leakage level by a factor of 3. Reducing the AlInN barrier thickness by 25 % results in a leakage level below 1 mA/mm which is expected to improve transistor robustness. At the same time, the RF gain increased by up to 1 dB while maintaining a good output power of 3.7 W/mm, which makes it the most promising candidate for further investigations.

REFERENCES

- [1] U. K. Mishra, I. Shen, T. E. Kazior, and Y. F. Wu, "GaN-based RF power devices and amplifiers" Proc. IEEE, vol. 96, no. 2, pp. 287-305, Feb. 2008.
- [2] S. Nagarajan, M. S. Kumar, Y. J. Choi, S. J. Chung, C.-H. Hong, and E.-K. Suh, "Al composition dependent structural and electrical properties of InAlGaN/GaN heterostructures", J. Phys. D: Appl. Phys. 40, 4653 (2007).
- [3] F. Medjoub, R. Kabouche, A. Linge, et al., "High electron mobility in high-polarization sub-10 nm barrier thickness InAlGaN/GaN heterostructure", Appl. Phys. Express 8, 101001 (2015).
- [4] L. R. Khoshtoo, N. Ketteniss, C. Mauder, H. Behmenburg, J. F. Woitok, I. Booker, J. Gruis, M. Heuken, A. Vescan, H. Kalisch, and R. H. Jansen, "Quaternary nitride heterostructure field effect transistors", Phys. Status Solidi C 7(7), pp. 2001-2003 (2010).
- [5] H. Behmenberg, L. R. Khoshroo, M. Eickelkamp, C. Mauder, M. Fieger, N. Ketteniss, J. Woitok, D. Wamwangi, M. Wuttig, S. E. Hernandez, T. Schäpers, M. Heuken, A. Vescan, H. Kalisch, and R. H. Jansen, "Influence of barrier thickness on AlInN/AlN/GaN heterostructures and device properties", Phys. Status Solidi C 6 (52), pp. 1041-1044 (2009).
- [6] S. Piotrowicz, O. Jardel, E. Chartier, R. Aubry, L. Baczkowski, M. Casbon, C. Dua, L. Escotte, P. Gamarra, J. C. Jaquet, N. Michel, S. D. Nsele, M. Oualli, O. Patard, C. Potier, M. A. Di-Forte Poisson, and S. L. Delage, "12 W/mm with 0.15 μ m InAlN/GaN HEMTs on SiC technology for K and Ka-band applications", IEEE MTT-S International Microwave Symposium (IMS2014).
- [7] J. M. Manuel, F. M. Morales, R. Garcia, T. Lim, L. Kirste, R. Aidam, and O. Ambacher, "Improved structural and chemical properties of nearly lattice-matched ternary and quaternary barriers for GaN-based HEMTs", Cryst. Growth Des. 11 (6), pp. 2588-2591 (2011).
- [8] O. Jardel, J.-C. Jaquet, L. Baczkowski, D. Carisetti, D. Lancereau, M. Olivier, R. Aubry, M.-A. Di Forte-Poisson, C. Dua, S. Piotrowicz, and S. L. Delage, "InAlN/GaN HEMTs based L-band high-power packaged amplifiers", International Journal of Microwave and Wireless Technologies 6(6), pp. 565-572 (2014).
- [9] M. Hiroki, Y. Oda, N. Watanabe, N. Maeda, H. Yokoyama, K. Kumakura, and H. Yamamoto, "Unintentional Ga incorporation in metalorganic vapor phase epitaxy of In-containing III-nitride semiconductors", J. Cryst. Growth 382, pp. 36-40 (2013).
- [10] J. Kim, M.-H. Ji, T. Detchprohm, R. D. Dupis, A. M. Fischer, F. A. Ponce, and J.-H. Ryou, "Effect of group-III precursors on unintentional gallium incorporation during epitaxial growth of InAlN layers by metalorganic chemical vapor deposition", J. Appl. Phys. 118, 125303 (2015).
- [11] Fang, J. Guo, Z. Hu, O. Laboutin, Y. Cao, W. Johnson, G. Snider, P. Fay, D. Jena, and H. Xing, "220 GHz quaternary barrier InAlGaIn/AlN/GaN HEMTs", IEEE Device Lett. Vol. 32(9), pp. 892-894 (2011).
- [12] N. Ketteniss, L. R. Khoshroo, M. Eickelkamp, M. Heuken, H. Kalisch, R. H. Jansen, and A. Vescan, "Study on quaternary AlInGaIn/GaN HFETs grown on sapphire substrates", Semicond. Sci. Technol. 25, 075013 (2010).
- [13] M. A. Khan, J. W. Yang, G. Simin, R. Gaska, M. S. Shur, H.-C. zur Loye, G. Tamulaitis, A. Zukauskas, D. J. Smith, D. Chandrasekhar, and R. Bicknell-Tassius, "Lattice and energy band engineering in AlInGaIn/GaN heterostructures", Appl. Phys. Lett. 76, 1161 (2000).
- [14] L. Kirste, T. Lim, R. Aidam, S. Müller, P. Waltereit, and O. Ambacher, "Structural properties of MBE AlInN and AlGaInN barrier layers for GaN-HEMT structures", Phys. Status Solidi A 207(6), pp. 1338-1341 (2010).
- [15] K. Makiyama, S. Ozaki, T. Ohki, et al. "Collapse-free power InAlGaIn/GaN-HEMT with 3 W/mm at 96 GHz", IEEE International Electron Device Meeting (IEDM), pp. 9.1.1-9.1.4 (2015).
- [16] Y. Liu, H. Jiang, S. Arulkumaran, T. Egawa, B. Zhang, H. Ishikawa, "Demonstration of undoped quaternary AlInGaIn/GaN heterostructure field-effect transistor on sapphire substrate", Appl. Phys. Lett. 86(22), 223510 (2005).
- [17] O. Ambacher, J. Majewski, C. Miskys, A. Link, M. Hermann, M. Eickhoff, M. Stutzmann, F. Bernardini, V. Fiorentini, V. Tilak, B. Schaff, and L. F. Eastman. "Piezoelectric properties of Al(In)GaIn/GaN hetero- and quantum well structures", J. Phys.: Condens Matter 14, pp. 3399-3434 (2002).
- [18] J. M. Manuel, F. M. Morales, R. Garcia, T. Lim, L. Kirste, R. Aidam, and O. Ambacher, "Improved structural and chemical properties of nearly lattice-matched ternary and quaternary barriers for GaN-based HEMTs", Cryst. Growth Des. 11, pp. 2588-2591 (2011).